A Dataset Augmentation Method for Non-convergent Power Flow Adjustment Behavior Based on Improved Conditional Generative Adversarial Network

Xin Wu[1*], Liang Zhang[1], Sheng Xu[2], Jiangfeng Qian[2], Qi Li[2]
[1]East China Branch, State Grid Corporation of China, Shanghai 200120, China
[2]State Grid Electric Power Research Institute (NARI Group Corporation) - NARI Technology Co., Ltd., Nanjing 211106, China
Corresponding author: Xin Wu (e-mail: wu_xin@ec.sgcc.com.cn).

ABSTRACT This paper proposes a data augmentation method for generating non-convergent power flow adjustment behavior datasets based on an improved generative adversarial network. Firstly, a mechanistic analysis of power flow non-convergence and adjustment strategies is conducted, and metrics for evaluating the non-convergent power flow adjustment behavior dataset are proposed. Secondly, the fundamental principles and architectural features of the Conditional Generative Adversarial Network (CGAN) and Long Short-Term Memory (LSTM) network are introduced. Then, a data-driven augmentation method for the non-convergent power flow adjustment behavior dataset is presented. By incorporating an extreme value theory mechanism, the training capability of the CGAN on the training data is enhanced. Furthermore, LSTM is embedded into the GAN framework to strengthen the learning and capture capability of multi-dimensional features during the non-convergent power flow adjustment process. Finally, case studies are used to validate the effectiveness of the proposed method. The generated dataset of non-convergent power flow adjustment behavior can effectively characterize the complete closed-loop process of a power grid transitioning from an ill-conditioned state back to a solvable state, providing a crucial training and verification foundation for power flow optimization practices.

INDEX TERMS Non-convergent Power Flow Adjustment; Conditional Generative Adversarial Network (CGAN); Long Short-Term Memory (LSTM); Data Augmentation

I. INTRODUCTION

I n steady-state analysis of power system, power flow calculation serves as a fundamental tool, whose convergence is directly critical to the accuracy and reliability of system operational state assessment [1-3]. However, with the large-scale integration of renewable energy, the increasingly complex structure of cross-regional interconnected grids, and system operating conditions approaching their limits, the non-convergence of power flow calculations occurs frequently. This has become a key bottleneck constraining power grid security analysis and operational decision-making [4-5]. Reference[6-7] presented a data-driven method for generating renewable scenarios using Generative Adversarial Networ(GAN). Reference[8] adopted Wasserstein Generative Adversarial Networks (WGAN) to learn the spatiotemporal correlations of renewable energy output, generating wind and solar stochastic scenarios that exhibit statistical similarity and pattern diversity. An improved model was proposed by incorporating an additional gradient penalty (GP) on the Wasserstein distance instead of using weight clipping in reference[9]. Reference [10] introduced a temporal correlation enhancement block into the GAN framework, which strengthens the temporal awareness of convolutional layers to generate wind power scenario sets for medium-to long-term timescales.Bayesian GANs are constructed and trained to produce a set of renewable power scenarios with the same pattern as historical data in reference[11].Reference [12] integrated Long Short-Term Memory (LSTM) structures, GAN, and deep learning methods to generate wind power scenarios, effectively capturing complex weather dynamics and temporal correlations in wind power output. Reference [13] utilized the active power data categorized by K-medoids clustering method to train a GAN model. Reference[14] presents an innovative approach that harnesses the power of both Recurrent Neural Networks (RNN) and GAN to revolutionize power generation forecasting in renewable energy systems. In recent years, GAN and their improved variants have emerged as mainstream approaches for data augmentation and sample generation. For the generation of datasets of non-convergent power flow adjustment behavior, Reference [15] proposed a deep learning method based on a physical power flow model to address the challenge of performing fast and accurate probabilistic power flow calculations. Reference [16] introduced a data augmentation method for non-convergent power flow adjustment behavior using a stacked denoising auto-encoder, which eliminates the need for time-consuming repeated power flow computations. Reference [17] presented a support vector machine-based approach to learn the dynamic mapping relationship between injected power and the non-convergent power flow adjustment process. Reference [18] implemented the generation of a non-convergent power flow adjustment behavior dataset considering injected power, branch power, and voltage by employing partial least squares and Bayesian linear regression methods. References [19] and [20] respectively utilized Back Propagation (BP) neural networks and Radial Basis Function (RBF) neural networks to approximate power flow equations, replacing traditional power flow data generation models and thereby accelerating the reinforcement of non-convergent power flow adjustment behavior data. Reference [21], targeting the difficulty of traditional power flow data augmentation methods in meeting the requirements for fast and accurate probabilistic power flow calculation, proposed a method that extracts power flow features based on extreme learning machines to accelerate the generation of samples for non-convergent power flow adjustment behavior data. However, existing data generation methods for non-convergent power flow adjustment behavior focus solely on improving the overall model accuracy during training, while certain power flow variables still exhibit anomalous errors. These abnormal deviations are manifested as significant inaccuracies in specific variables, even when the data-driven model's overall precision meets training expectations. Excessive errors in some variables can severely compromise the reliability of generated samples of non-convergent adjustment behavior in grid applications, potentially leading to misjudgments, such as incorrect identification of power flow limit violations, threatening the secure and stable operation of the power system. This paper proposes a dataset augmentation method for non-convergent power flow adjustment behavior based on an improved Conditional Generative Adversarial Network (CGAN). First, a metric indicator system for the non-convergent power flow adjustment behavior dataset is construted based on the mechanistic analysis of power flow non-convergence and adjustment strategies. Second, the core principles and architectural characteristics of the CGAN and LSTM network are examined. Then, a data-driven augmentation scheme for the non-convergent power flow adjustment behavior dataset is presented. This scheme employs an Extreme Value Theory-embedded Conditional Generative Adversarial Network (EVT-CGAN) to enhance the training data, thereby accelerating the convergence efficiency of the sample generation process, and LSTM is embedded into the CGAN framework to strengthen the model's ability to learn and capture the dynamics of the non-convergent power flow adjustment process. Finally, the effectiveness of the proposed method is validated through case studies.

II. MECHANISTIC ANALYSIS OF POWER FLOW NON-CONVERGENCE

A. MATHEMATICAL INTERPRETATION OF POWER FLOW NON-CONVERGENCE

Power flow calculation is inherently a process of solving nonlinear equations, whose convergence critically depends on the uniqueness of the solution, the reasonableness of the initial value selection, and the numerical stability of the algorithm. As the mainstream algorithm, the Newton-Raphson method linearizes the power flow equations through Taylor expansion, with its iterative scheme expressed as:

$$\Delta x^{(k)} = J^{-1}\left(x^{(k)}\right) \cdot f\left(x^{(k)}\right)$$

where J is the Jacobian matrix, and f(x) is the power mismatch vector. The convergence of the Newton-Raphson method is highly sensitive to the selection of the initial guess. When the initial value $x^{(0)}$ is far from the true solution, the iterative process is prone to fall into local oscillation or divergence, especially when the Jacobian matrix becomes near-singular, as the computed correction step becomes ill-conditioned, ultimately leading to algorithmic failure.

Mathematically, the ill-conditioning of the Jacobian matrix,namely, "ill-conditioned power flow," is a key factor leading to non-convergence. When the matrix condition number is excessively large, minor numerical errors can cause drastic fluctuations in the correction steps. As the system operating point approaches the static voltage stability limit, the Jacobian matrix becomes ill-conditioned, resulting in the failure of solving the correction equations during the Newton-Raphson iterative process. Particularly under heavily loaded conditions, the power-voltage sensitivity coefficients increase sharply, and the eigenvalue distribution of the Jacobian matrix tends to diverge, forming a numerically infeasible region.

The absence of real-number solutions to the power flow equations further exacerbates the convergence difficulty. As load increases, the number of power flow solutions decreases in a pairwise manner until no real-number solutions exist, indicating that the system operating point lies outside the feasible region.

Furthermore, under operating conditions that violate operational constraints—such as voltage limit violations or power imbalance—the mathematical manifestation is a sudden change in the structure of the solution space, namely, the system operating point crossing the stability boundary and entering an infeasible region. Concurrently, the system may possess multiple operating solutions. Conventional iterative algorithms are prone to becoming trapped in local convergence basins, thereby failing to reach the physically realistic solution. This phenomenon is particularly pronounced in distribution networks exhibiting dual-solution characteristics.

B. FEATURE SET OF THE NON-CONVERGENT POWER FLOW ADJUSTMENT PROCESS

Focusing on the construction of feature indicators for the dataset of non-convergent power flow adjustment behavior, this work aims to provide more precise data support for power system analysis and optimization. To address the error accumulation and decision-making bias caused by non-convergence issues in traditional power flow calculations, multi-source information—including grid topology, equipment parameters, and operational states—is integrated to build a high-dimensional dataset encompassing both static features and dynamic behaviors.

First, based on the dynamic response characteristics of electrical parameters, core indicators such as voltage deviation rate, power angle oscillation amplitude, and line load margin are extracted to quantify the transient changes in system states during the adjustment process. The voltage deviation rate is defined as the relative change in node voltage magnitude before and after adjustment, while the power angle oscillation amplitude is calculated as the standard deviation of phase angle differences to capture the evolution pattern of stability.

Second, for the sequence of adjustment behaviors, time-series feature indicators are constructed, including adjustment action trigger frequency, response delay time, and power correction gradient. Sliding window analysis is employed to reveal the periodicity and burstiness of behavioral patterns. Furthermore, statistical distribution features—such as the skewness, kurtosis, and information entropy of adjustment quantities—are introduced to evaluate the concentration and uncertainty of behavioral distributions.

The core feature metric set

$$R_i = \{P_{\max,i}, P_{\text{ave},i}, P_{\text{flu},i}, T_{p,i}\}$$

is constructed by selecting the maximum/minimum per-unit values, fluctuation rate (standard deviation of the power change rate between adjacent time steps), and anomaly duration during the power flow recovery process, in order to characterize the differentiated dynamic features of the non-convergent power flow adjustment behavior dataset. Here, the fluctuation rate is expressed as:

$$P_{\text{flu}} = \sum_{t=2}^{T} \frac{|P_t - P_{t-1}|}{T-1}$$

where P_t and P_{t-1} denote the power flow at time t and the preceding time step $t-1$, respectively, and T represents the total sample duration.

Based on the extracted feature metric set of non-convergent power flow adjustment behavior, conditional inputs are fed into the generator model to guide its learning of the mapping relationship between adjustment actions and the dynamic characteristics of power flow.

III. CONDITIONAL GENERATIVE ADVERSARIAL NETWORK MODEL AND ITS IMPROVEMENTS

A. CONDITIONAL GENERATIVE ADVERSARIAL NETWORK (CGAN)

Given that non-convergent power flow adjustment is constrained by multidimensional conditions, a CGAN is employed. By introducing a conditional information embedding mechanism, the multi-factor labels of non-convergent power flow adjustment are incorporated as a conditional vector, and prior constraints are added on both the generator and the discriminator, thereby achieving conditional guidance throughout the data generation process [22]. The network structure is illustrated in Figure 1.

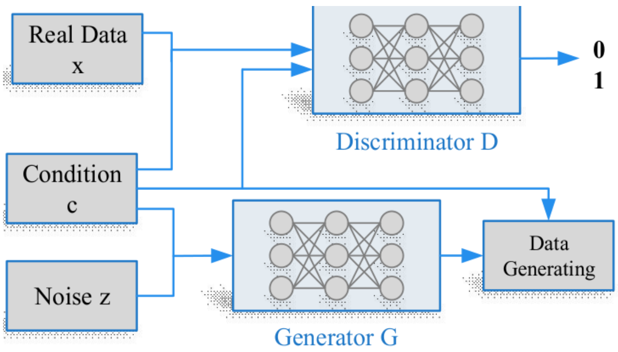

FIGURE 1. Basic structure of CGAN

CGAN achieves conditionally guided sample generation and discrimination through adversarial optimization [23]. The generator G takes a latent noise vector z and a conditional variable c as inputs, producing a synthetic sample x' = G(z|c) via nonlinear mapping. Subsequently, the condition c is concatenated with both the real sample x and the generated sample x', respectively, before being fed into the discriminator D to evaluate the proximity between the probability distributions of the generated and real data. The generator aims to ensure that x' approximates the real sample x as closely as possible under the constraint of condition c; whereas the discriminator strives to maximize the distinguishability between x and x' while ensuring that x' conforms to condition c. The loss functions for the generator and discriminator, along with the overall training objective function of the CGAN, are formulated as:

$$\begin{aligned}
\text{Loss}_G &= -E_{x' \sim p(x')}[D(x'|c)] \\
\text{Loss}_D &= -E_{x \sim p(x)}[D(x|c)] \\
&\quad + E_{x' \sim p(x')}[D(x'|c)] \\
\min_G \max_D V(D,G) &= E_{x \sim p(x)}[D(x|c)] \\
&\quad - E_{x' \sim p(x')}[\log(1 - D(x'|c))]
\end{aligned}$$

where E denotes the expectation operator, and p(x) and p(x') represent the probability distributions of the real samples and the generated samples, respectively.

B. EXTREME VALUE THEORY (EVT)

Extreme Value Theory (EVT) employs mathematical models to characterize the extreme deviation properties and the asymptotic tail behavior of probability distributions, enabling the quantitative analysis of extreme event probabilities and the extrapolation of extreme scenarios beyond the observed sample data. The Generalized Pareto Distribution (GPD), which integrates the core characteristics of the heavy-tailed Pareto distribution and the light-tailed exponential distribution, can accurately describe the probability distribution patterns of extreme values in random variables [24]. Its cumulative distribution function is expressed as:

$$G_{\sigma,\xi}(x) = \begin{cases} 1 - \left(1 + \dfrac{\xi x}{\sigma}\right)^{-1/\xi}, & \xi \neq 0, \\ 1 - \exp\left(-\dfrac{x}{\sigma}\right), & \xi = 0. \end{cases}$$

where σ and ξ represent the scale parameter and shape parameter, respectively.

For the multidimensional small-probability or extreme variables in the context of non-convergent power flow adjustment, the Peaks Over Threshold (POT) method is adopted to extract extreme data exceeding a critical threshold for constructing the tail model. A sufficiently high threshold satisfying asymptotic extremal properties (typically set at the 95% quantile level) is defined. Under this condition, the distribution of the excess sequence x-u is characterized by the GPD, with its shape and scale parameters estimated via maximum likelihood estimation:

$$\lim_{u \to \bar{x}} \sup_{0 \leq x < \bar{x} - u} \left| F_u(x) - G_{\sigma(u),\xi}(x) \right| = 0$$

where u denotes the threshold, $\bar{x}$ represents the right endpoint of the distribution, and F_u is the excess distribution function defined as:

$$F_u(x) = P(X - u \leq x \mid X > u).$$

C. LONG SHORT-TERM MEMORY NETWORK (LSTM)

LSTM network integrates a gating system comprising a forget gate, an input gate, and an output gate, thereby constructing a neuron structure endowed with dynamic memory capability.

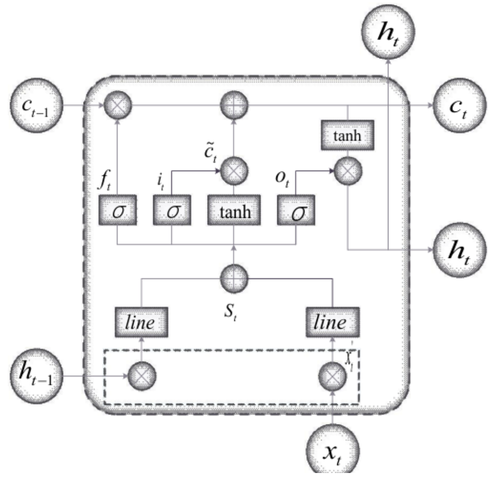

FIGURE 2. LSTM basic unit structure

Configuring input data $x_1, x_2, \ldots, x_t$, inputing vector x_t at time t, and conducting a parameterized linear transformation with the hidden unit from the previous time step h_{t-1}, the current hidden unit h_t is generated.

The forget gate, based on the current input and the previous hidden state, generates a control signal within the range [0, 1] through a Sigmoid activation function. This signal quantifies the extent to which information from the previous memory cell state is retained or discarded. When the output approaches 1, the memory cell state is fully preserved; when it approaches 0, historical information is selectively forgotten. This mechanism effectively mitigates the gradient vanishing problem [25].

$$f_t = \mathrm{sigmoid}(w_{xf}x_t + w_{hf}h_{t-i} + b_f)$$

where f_t denotes the output of the forget gate at time step t, and W_f and b_f represent the weight matrix and the bias term of the forget gate, respectively.

The input gate operates through the coordinated action of a Sigmoid layer and a tanh layer. The former generates weighting coefficients for information updates, while the latter produces a candidate vector. These two components are then multiplied element-wise to form the new information to be injected into the memory cell at the current time step. This mechanism effectively filters out noise interference from the input data, selectively integrates salient features into the memory cell, and thereby enhances the network's capability to characterize the complex data flow associated with non-convergent power flow adjustment.

$$\begin{aligned} i_t &= \mathrm{sigmoid}(w_{xi}x_t + w_{hi}h_{t-i} + b_i) \\ \bar{C}_t &= \tanh(w_{xc}x_t + w_{hc}h_{t-i} + b_c) \end{aligned}$$

where i_t denotes the output of the forget gate at time step t, $[W_{hi}, W_{xi}]$ and b_i represent the weight matrix and bias term of the forget gate, respectively, $\bar{C}_t$ is the candidate memory cell content generated at the current time step, w_{xc} is the weight matrix used to compute the candidate memory cell content, and b_c is the corresponding bias term.

The output gate also employs a Sigmoid activation function to generate output weighting coefficients based on the updated memory cell state. These coefficients are then combined with the memory information from tanh transformation, dynamically regulating the output of the hidden state at the current time step. Leveraging the synergistic action of the gating mechanisms, the LSTM can effectively model long-range temporal dependencies. Through selective flow and storage of information, it significantly enhances robustness and feature representation capability in complex non-convergent power flow adjustment tasks.

$$
\begin{aligned}
C_t &= f_t \otimes C_{t-1} + i_t \otimes \bar{C}_t \\
o_t &= \mathrm{sigmoid}(w_{xo}x_t + w_{ho}h_{t-i} + b_o) \\
h_t &= o_t \tanh(C_t)
\end{aligned}
$$

where o_t denotes the output value of the output gate, $[W_{ho}, W_{xo}]$ and b_o represent the weight matrices and bias term, respectively.

IV. DATASET AUGMENTATION METHOD FOR NON-CONVERGENT POWER FLOW ADJUSTMENT BEHAVIOR

A. DATASET AUGMENTATION FRAMEWORK NON-CONVERGENT POWER FLOW ADJUSTMENT BEHAVIOR

To enhance the model's feature extraction capability for the temporal characteristics of non-convergent power flow adjustment behavior indicators, an EVT-LSTM-CGAN-based augmentation model for non-convergent power flow adjustment behavior datasets is proposed, with its framework illustrated in Figure 3.

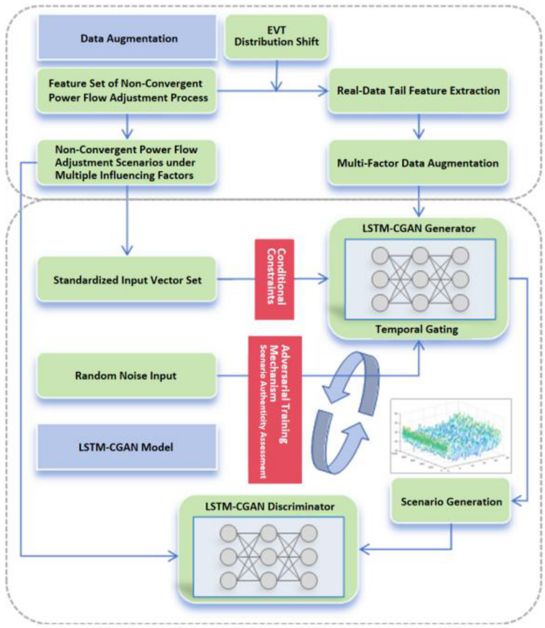

FIGURE 3. Dataset augmentation framework for the non-convergent power flow adjustment behavior based on LSTM-CGAN

The core of the framework lies in establishing a mapping relationship between non-convergent power flow adjustment behavior and the dataset encompassing the entire adjustment process. The adversarial training mechanism ensures the distributional fidelity of generated samples, while the temporal gating units extract dependency relationships within data sequences, achieving joint optimization of data generation quality and temporal dependency modeling.

First, a distribution shifting algorithm based on EVT is designed to extract tail characteristics from historical data, thereby augmenting samples of non-convergent power flow adjustment behavior and mitigating the scarcity of low-probability event samples. Second, LSTM networks are embedded into both the generator and discriminator structures of the CGAN to strengthen dynamic feature modeling and capture long-range dependencies during the power flow recovery process. Subsequently, a quantitative feature metric system for non-convergent power flow adjustment behavior data is constructed. This system establishes a quantitative mapping between the adjustment process and the behavioral dataset, generating a standardized input vector set to provide interpretable guiding parameters for the generator. Finally, a "Conditional Parameter–Feature Mapping–Scenario Generation" architecture is established. Through conditionally constrained adversarial generative training, it achieves the targeted generation of scenario-specific samples for the non-convergent power flow adjustment behavior dataset.This framework, via the synergistic mechanism of data augmentation, temporal modeling, and conditional constraints, accomplishes the enhancement of both the non-convergent power flow adjustment behavior and the dataset covering the complete adjustment process.

B. DATA AUGMENTATION FOR NON-CONVERGENT POWER FLOW ADJUSTMENT BEHAVIOR

An iterative extreme data augmentation method is proposed, which integrates EVT and CGAN to construct an extreme-value-oriented distribution transformation model. This model enhances the adversarial network's capability to model anomalous scenarios by shifting data features toward the extreme-value domain and reconstructing the probability space of historical data. Here, EVT is employed to model the tail characteristics of the data, while CGAN is responsible for achieving high-dimensional distribution matching.

First, the Peaks Over Threshold (POT) method is employed to extract extreme samples from historical data, based on which a GPD is fitted. Subsequently, synthetic data are generated using a CGAN and iteratively concatenated with the original data, progressively shifting the overall data distribution toward the tail characteristics of the GPD, thereby achieving effective augmentation of extreme data.

Given a dataset containing n samples, they are first sorted in descending order according to an extreme-value metric. The top c·n extreme samples are selected to form the initial training set. A CGAN is trained on this subset to generate [(n-cn)/c] candidate samples. Similarly, by applying extreme-value screening to these candidates, n-c·n samples are retained and merged with the initial extreme samples to form the training set for the next iteration. During training, a parameter inheritance strategy is adopted, where the generator's network parameters from the current round are used as the initial values for the next round of training, significantly improving training efficiency. Through this iterative optimization process, the distribution of the generated data progressively approximates the theoretical extreme tail distribution while ensuring training stability.

C. DATASET GENERATION FOR NON-CONVERGENT POWER FLOW ADJUSTMENT BEHAVIOR

The LSTM mechanism is introduced to enhance the EVT-CGAN data augmentation model. Specifically, LSTM is employed to extract implicit features from non-convergent power flow adjustment behavior data, namely the trend information that evolves with multi-dimensional factors and is difficult to quantify. The LSTM architecture processes input data through temporal iteration, outputting fixed-length feature vectors at each time step. These hidden states serve as conditional inputs to the generative network to drive the synthesis of sequential data. The model as a whole relies on CGAN to generate new content while utilizing LSTM to accomplish implicit feature learning.

$$\begin{aligned} v_{n+1} &= \arg\max_{v_{n+1}} P(v_{n+1} \mid \tilde{v}_{n-j+1}, \tilde{v}_{n-j+2}, \ldots, \tilde{v}_n) \\ &= \arg\max_{x} P(G(z) \mid \tilde{v}_{n-j+1}, \tilde{v}_{n-j+2}, \ldots, \tilde{v}_n) \\ &\approx \arg\max_{x} P(G(z) \mid f_{\mathrm{lstm}}(\tilde{v}_{n-j+1}, \tilde{v}_{n-j+2}, \ldots, \tilde{v}_n)) \\ &\approx G(h_t) \end{aligned}$$

where v_{n+1} denotes the predicted value or output at time step $n+1$; argmax indicates the parameter or state when v_{n+1} takes the maximum probability; $P(v_{n+1}|\tilde{v}_{n-j+1}, \tilde{v}_{n-j+2}, \ldots, \tilde{v}_n)$ is the conditional probability representing the prediction of the output at time step $n+1$ given the data from the past j time steps; f_{LSTM} is the LSTM function (or model) that processes historical data and produces a fixed-dimensional vector representation; $\tilde{v}_n$ represents the actual observed historical data points; and h_t denotes the hidden state of the LSTM at time t, which serves as the final input to the generator.

The generator receives two core inputs: first, the temporal feature vector extracted from historical data by the LSTM network; second, artificially configured extreme condition parameters, encompassing a multi-dimensional indicator vector that characterizes the behavior under non-convergent power flow adjustment.

The model workflow comprises two core stages: temporal feature encoding and conditional generation. In the temporal feature encoding stage, an LSTM network is employed to perform temporal feature extraction on the input conditional sequence of non-convergent power flow adjustment behavior. Leveraging its gating mechanisms, the LSTM captures dependencies between time steps and compresses the variable-length sequence into a fixed-dimensional semantic vector, thereby achieving a high-level semantic representation of the adjustment behavior. A dual-hidden-layer structure is utilized to reduce data redundancy and handle the non-stationarity and long-range dependencies inherent in non-convergent power flow adjustment behavior data. The output latent vector carries scene-variation driving information and serves as a condition vector imbued with temporal context for the generator.

During the conditional generation and adversarial learning stage, the feature vector output by the LSTM is concatenated with a random noise vector and fed into the generator. The generator, through multiple layers of nonlinear transformations, produces scenario sequences that conform to specific non-convergent power flow adjustment behaviors. Simultaneously, the discriminator receives both real and generated scenario data of non-convergent power flow adjustment behavior. Through adversarial training, the generator parameters are optimized to encourage the generated data to closely match the real data in terms of statistical distribution, temporal characteristics, and conditional labels. The CGAN explicitly controls the generation process via conditional signals, enabling the targeted synthesis of different non-convergent power flow adjustment behavior scenarios.

To address the issues of gradient competition where the generator dominates optimization) and reduced feature extraction efficiency due to information redundancy, which arise during joint training when the generator has more parameters than the LSTM encoder, a phased optimization strategy is adopted during training to balance generation quality and feature learning. In the first phase, the CGAN generator is trained separately to learn the fundamental distribution patterns of the non-convergent power flow adjustment behavior dataset. In the second phase, the generator parameters are fixed, and training focuses on the LSTM network to uncover latent driving factors. This approach mitigates the dominance problem caused by the generator's numerical advantage in neuron count and enhances the model's interpretability regarding the change mechanisms of non-convergent power flow adjustment behavior.

D. ACCURACY EVALUATION METRIC SYSTEM FOR SAMPLE AUGMENTATION

A multi-dimensional comprehensive evaluation framework encompassing data augmentation accuracy, uncertain feature fitting, and low-probability tail characterization efficacy is constructed. Each evaluation metric [26-27] is based on the sample statistical mean, and a lower metric value indicates a higher degree of alignment between the distribution of generated samples and the ground truth, signifying superior model performance.

1) Energy Score (ES)

ES constructs a quantitative assessment framework for distributional differences between generated and real data by integrating fitting-error and diversity-error metrics, thus,suitable for evaluating the performance of data augmentation and sample generation models.

$$ES = P_j \sum_{j=1}^{N} \left\| Z_t - \widehat{Z}_t^{(j)} \right\|_2 - \frac{1}{2} P_i P_j \sum_{i=1}^{N} \sum_{j=1}^{N} \left\| \widehat{Z}_t^{(i)} - \widehat{Z}_t^{(j)} \right\|_2$$

where P_i and P_j denote the probabilities of generated scenarios i and j, respectively; and Z_t, $\widehat{Z}_t^{(i)}$, $\widehat{Z}_t^{(j)}$ represent the real non-convergent power flow adjustment behavior dataset at time t, and the corresponding datasets for scenarios i and j, respectively.

2) Continuous Ranked Probability Score (CRPS)

The CRPS quantifies the discrepancy between the cumulative distribution of generated samples and the true probability distribution, thereby evaluating the calibration performance of the data augmentation method.

$$CRPS = \frac{1}{T} \sum_{t=1}^{T} \left(\frac{1}{N} \sum_{i=1}^{N} |s_{i,t} - P_{real,t}| - \frac{1}{2N^2} \sum_{i,j=1}^{N} |s_{i,t} - s_{j,t}| \right)$$

where $s_{i,t}$ and $s_{j,t}$ denote the non-convergent power flow adjustment behavior datasets of the i-th and j-th generated scenarios at time t, respectively.

3) Variogram Score (VS)

VS constructs an evaluation framework for assessing the fitting accuracy of correlation structures between augmented generated samples and real data by quantifying the differences in variability at different lag distances.

$$VS = \sum_{t=1}^{T} \left(|P_{real,t} - P_{real,t'}|^{1/2} - \frac{1}{W} \sum_{w=1}^{W} |s_{w,t} - s_{w,t'}|^{1/2} \right)^2$$

where $P_{real,j}$ denotes the real non-convergent power flow adjustment behavior dataset at time j; $s_{w,t}$ and $s_{w,t'}$ represent the generated non-convergent power flow adjustment behavior datasets of the w-th scenario at times t and t', respectively.

4) Pinball Score (PS)

The PS metric establishes a validation mechanism for the effectiveness of the generation method by measuring the absolute deviation between quantiles of the generated sequence and the actual values.

$$PS = \frac{1}{T} \sum_{i=t+1}^{t+T} (P_i, Q_i) = \begin{cases} (\mu_c - 1)(P_{real,i} - Q_{\mu_c,i}), & P_{real,i} < Q_{\mu_c,i}, \\ \mu_c(P_{real,i} - Q_{\mu_c,i}), & P_{real,i} \geq Q_{\mu_c,i}. \end{cases}$$

where μ_c is the value of the sample cumulative distribution function, taken at intervals of 0.05; $P_{real,i}$ and $Q_{\mu_c,i}$ denote the measured value of the non-convergent power flow adjustment behavior dataset at time i and the corresponding generated value at the μ_c-quantile, respectively.

5) Autocorrelation Coefficient (ACC)

The AC assesses the consistency of temporal statistical characteristics between the augmented generated power flow dataset and the measured power flow data by evaluating the correlation of temporal outputs over

$$AC(\tau) = \frac{E[(S_t - \mu)(S_{t+\tau} - \mu)]}{\sigma^2}$$

where S denotes the temporal data, μ and σ are the mean and variance of the sequence, τ represents the time lag, and E denotes the expected value of the power flow difference.

V. CASE STUDY

A. CASE SETTING

An empirical analysis is conducted using power flow simulation and non-convergent adjustment data from a high renewable-penetration region in East China, effectively mitigating the interference of geographical and environmental disparities on model training. A training set is constructed based on a typical dataset of non-convergent power flow adjustment behavior, followed by feature engineering and model parameter optimization. Simultaneously, a portion of the data is reserved as a test set to enable quantitative validation of the effectiveness of the data augmentation method.

The empirical analysis follows a technical pathway of "Data Preprocessing – Model Training – Scenario Generation – Effectiveness Verification – Comparative Analysis." Based on the scenario accuracy evaluation metric system, a quantitative assessment of the generation method is conducted. By comparing the proposed dataset augmentation model for non-convergent power flow adjustment behavior with samples generated by CGAN and LSTM-CGAN, the analysis reveals the significant advantages of the proposed model in handling datasets of non-convergent power flow adjustment behavior.

B. GENERATION AND PERFORMANCE EVALUATION OF TYPICAL SCENARIOS

Holding out a portion of the dataset from model training serves to effectively validate the robustness of the generative model. Typical power flow scenario data are selected as input for training, while the test set comprises measured data. Visual comparisons are conducted between randomly generated samples and the test set.

The heavy-load operating scenario is interpreted as a condition where the system load level approaches or exceeds the transmission network's transfer limit, often leading to non-convergence in power flow calculations. Specific manifestations include: concentrated regional loads and excessive power demand at load centers, causing power flow limits on relevant transmission interfaces to be violated; limited generator outputs, with critical units reaching their capacity ceilings and unable to provide sufficient power support; and deteriorating voltage stability, where voltage magnitudes at load nodes continuously drop beyond acceptable operational ranges.

High penetration of renewable energy introduces distinctive non-convergence issues. For example, abrupt fluctuations in renewable power output induce drastic changes in power flow distribution; system frequency stability declines, and power-angle oscillations intensify.

This paper selects the above scenarios as the validation baseline for the dataset augmentation model of non-convergent power flow adjustment behavior. This approach effectively assesses the model's capability to capture and interpret the correlated features within complex non-convergent adjustment data, provides a more comprehensive evaluation of model robustness and generalization performance, and offers higher representativeness and demonstrative power.

Figure 4 presents a comparison between randomly selected generated samples and test samples under the heavy-load operating scenario. Compared with the actual scenario values, the generated non-convergent power flow adjustment behavior data exhibit no significant deviation or fluctuation, maintaining highly similar dynamic characteristics. Furthermore, the value range of the generated scenarios fully covers that of the actual samples, indicating that the proposed method can effectively achieve sample augmentation that preserves the essential characteristics of the non-convergent power flow adjustment behavior dataset.

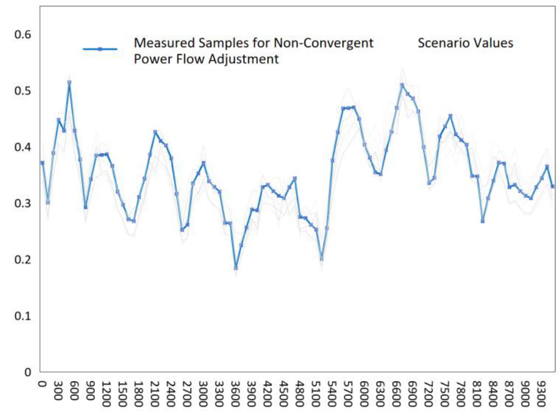

FIGURE 4. Comparison between randomly generated samples and measured samples under heavy-load operation scenarios

C. COMPARATIVE ANALYSIS OF GENERATED SCENARIOS

The construction of the scenario evaluation system prioritizes two dimensions: dispatch practicality and data-fitting accuracy. Focusing on the core requirements of power flow simulation, it systematically compares power flow characteristic parameters under extreme operating conditions. As shown in Tables 1-2, the synthesized data achieve over 90% consistency in key feature indicators under critical scenarios, confirming the model's generation efficacy in complex power flow adjustment scenarios.

TABLE 1. Accuracy of power flow characteristic indicators for generated samples under heavy-load operating scenarios (%)

Method	P_{max}	P_{min}	P_{flu}	T_p
CGAN	94.5	94.3	91.8	91.9
LSTM-CGAN	96.6	97.0	93.7	94.4
LSTM-EVT-CGAN	97.0	97.1	95.2	94.7

TABLE 2. Accuracy of power flow characteristic metrics for generated samples under high renewable-penetration scenarios (%)

Method	P_{max}	P_{min}	P_{flu}	T_p
CGAN	93.6	90.4	89.7	90.1
LSTM-CGAN	94.9	94.0	92.8	91.9
LSTM-EVT-CGAN	95.4	95.5	93.3	92.5

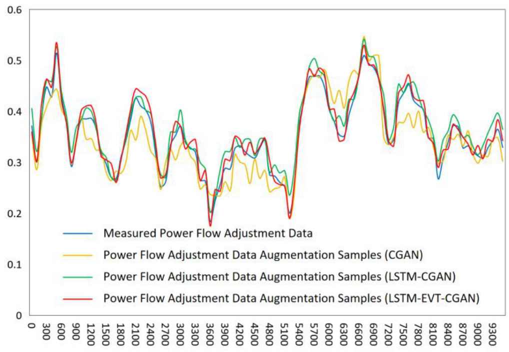

FIGURE 5. Comparison between randomly generated samples and measured power flow samples under heavy-load operating scenarios

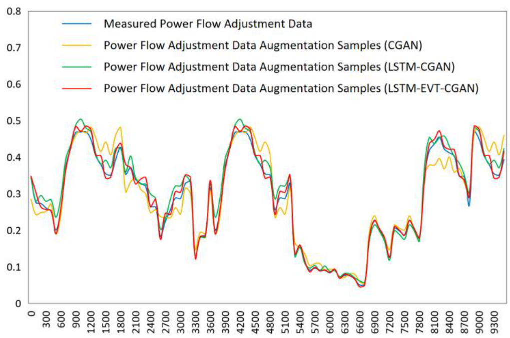

FIGURE 6. Comparison between randomly generated samples and measured power flow samples under high renewable-penetration scenarios

Figures 5 and 6 present the matching of dynamic characteristics between generated samples and independent test samples. The concordance analysis demonstrates that the proposed method effectively extracts implicit features of the power flow recovery process and accurately reproduces the key data characteristics of non-convergent power flow adjustment behavior in typical scenarios.

To thoroughly validate model performance, a multi-dimensional evaluation metric system is constructed to quantitatively assess the temporal features and statistical properties of the generated samples. As shown in Tables 3-4, compared to the baseline models CGAN and LSTM-CGAN, the proposed LSTM-EVT-CGAN exhibits significant advantages across key evaluation metrics, confirming its superior modeling capability in complex power flow adjustment scenarios.

TABLE 3. Evaluation metrics for generated samples under heavy-load operating scenarios

Method	ES	CRPS	VS	PS
CGAN	0.427	0.049	9.625	0.065
LSTM-CGAN	0.405	0.041	9.422	0.060
LSTM-EVT-CGAN	0.314	0.033	9.071	0.049

TABLE 4. Evaluation metrics for generated samples under high renewable-penetration scenarios

Method	ES	CRPS	VS	PS
CGAN	0.379	0.043	8.662	0.056
LSTM-CGAN	0.363	0.036	8.401	0.052
LSTM-EVT-CGAN	0.288	0.025	8.330	0.043

Given the isomorphic nature of the dataset augmentation and generation pipeline for non-convergent power flow adjustment behavior, and considering the representative research value of power flow mismatch issues under high renewable-penetration scenarios, this type of scenario is selected as the core research subject. For the three generative models—CGAN, LSTM-CGAN, and LSTM-EVT-CGAN—the box plots of the AC between their constructed non-convergent power flow adjustment behavior datasets and the measured temporal output (Figures 7 - 9) demonstrate that the synthetic data achieve a higher goodness-of-fit in temporal correlation with the measured data. This verifies the models' capability to accurately reproduce the statistical characteristics of complex power flow adjustment behavior.

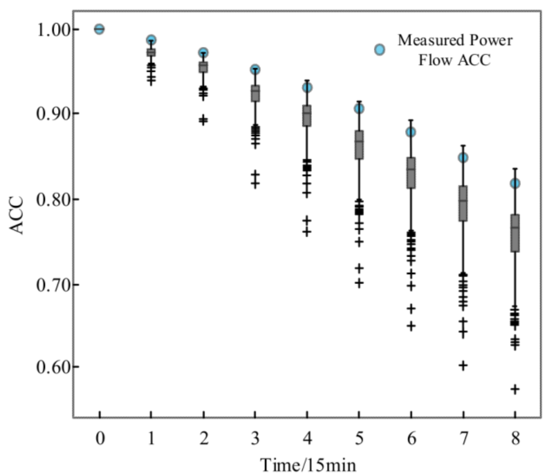

FIGURE 7. Box plot of ACC between scenario sample sets generated by CGAN and measured power flow samples

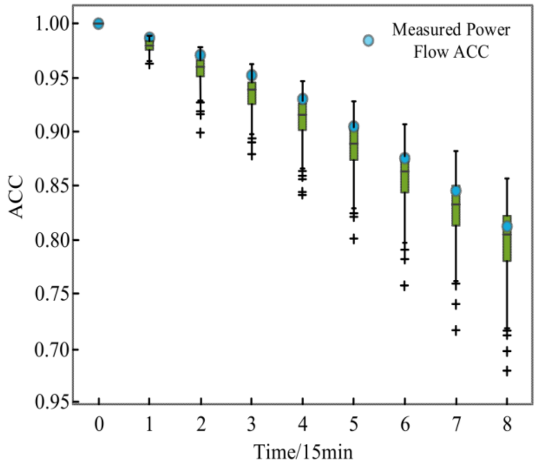

FIGURE 8. Box plot of ACC between scenario sample sets generated by LSTM-CGAN and measured power flow samples

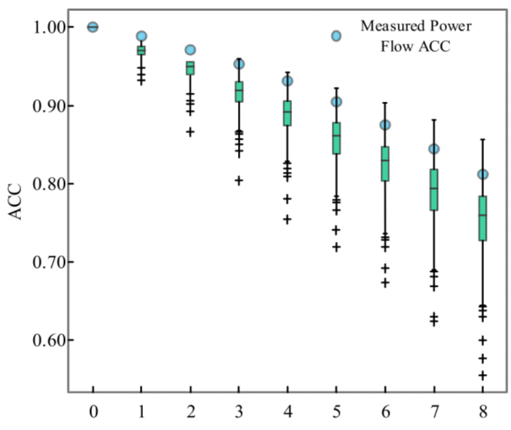

FIGURE 9. Box plot of ACC between scenario sample sets generated by LSTM-EVT-CGAN and measured power flow samples

The autocorrelation coefficient (ACC) of samples generated by the conventional CGAN shows a significant deviation from the measured sequence, reflecting its limited capability in modeling power flow dynamic correlations. In contrast, the ACC of scenario samples generated by LSTM-CGAN and LSTM-EVT-CGAN can cover the range of the measured sample ACC and exhibit strong consistency in variation patterns. Further analysis reveals that the proportion of ACC outliers in samples generated by the LSTM-enhanced CGAN models is significantly lower than that in the conventional CGAN, validating the enhancing effect of LSTM on the temporal modeling ability of the generator-discriminator pair. Notably, the median ACC of extreme scenario samples generated by LSTM-EVT-CGAN is closer to the ACC of the measured temporal output and shows a lower degree of deviation. This confirms that the extreme value theory-driven data augmentation strategy can effectively improve the model's learning efficiency for temporal correlations during the power flow recovery process and strengthen its capacity to characterize complex temporal dependencies.

It is worth noting that the sample augmentation effect under heavy-load operating scenarios is slightly superior to that under high renewable-penetration scenarios, rooted in the differences in the underlying data generation mechanisms. The former exhibits pronounced daily periodicity and nonlinear unimodal characteristics, with power flow feature distributions being relatively concentrated, allowing the model to capture stable mapping relationships from historical data more easily. The latter, however, is jointly influenced by spatiotemporally stochastic meteorological variables; the temporal fluctuations of power flow contain more non-stationary, multi-scale coupled complex features, requiring the learning of more intricate multivariate conditional mappings. This imposes higher demands on the model's ability to capture long-range dependencies and high-dimensional nonlinear dynamics.

VI. CONCLUSION

Focusing on the shortcomings of traditional power flow sample generation methods in implicit feature extraction and the lack of interpretability in generated scenarios, this paper proposes a dataset augmentation method for non-convergent power flow adjustment behavior based on an improved CGAN. By integrating EVT with the CGAN, a data augmentation framework is constructed. The developed feature metric system for the non-convergent power flow adjustment behavior dataset as conditional input, an enhanced CGAN model for dataset augmentation is designed, improved via LSTM networks. Validation through case studies leads to the following conclusions:

1) The data augmentation method integrating EVT and CGAN effectively addresses the scarcity of samples for non-convergent power flow adjustment behavior and significantly improves model training efficiency. By optimizing both the generation and discrimination processes with LSTM, and simultaneously constructing a feature vector set to enhance the generator's ability to map the association between typical non-convergent power flow scenarios and the adjustment behavior dataset, the method achieves feature-oriented generation of the non-convergent power flow adjustment behavior dataset.

2) The proposed model efficiently extracts implicit features from non-convergent power flow adjustment behavior data, enhancing its learning efficacy for temporal dynamic characteristics. Consequently, the accuracy rates of both the scenario evaluation metrics and the power flow characteristic indicators for the generated samples corresponding to non-convergent adjustment behavior are improved. The sample sets of the non-convergent power flow adjustment behavior dataset generated by the model for various typical non-convergent power flow scenarios can more reasonably characterize extreme power flow recovery properties. Compared with the conventional CGAN model, it demonstrates higher generation quality and stronger interpretability.

ACKNOWLEDGEMENT

Not applicable.

AUTHOR CONTRIBUTIONS

The authors confirm contribution to the paper as follows: Xin Wu, Liang Zhang: Conceptualization, data curation, formal analysis; Sheng Xu, Jiangfeng Qian, Qi Li: funding acquisition, investigation, methodology, project administration, resources, software; Xin Wu: supervision, validation, visualization, writing—original draft, writing—review and editing. All authors reviewed the results and approved the final version of the manuscript.

AVAILABILITY OF DATA AND MATERIALS

The data that support the findings of this study are available from the corresponding author on reasonable request.

ETHICS APPROVAL

Not applicable.

CONFLICTS OF INTEREST

The authors declare no conflicts of interest to report regarding the present study.

FUNDING STATEMENT

This work was supported by the Science and Technology Project of East China Branch of State Grid Co., LTD (No.: 52992425000U).

REFERENCES

[1] S. Talebi and K. Zhou, "Graph neural networks for efficient AC power flow prediction in power grids," *Electr. Eng. Syst. Sci.*, 2025, doi: 10.48550/arXiv.2502.05702.

[2] S. Wu, W. Hu, Z. Lu, et al., "Power system flow adjustment and sample generation based on deep reinforcement learning," *J. Mod. Power Syst. Clean Energy*, vol. 8, no. 6, pp. 1115–1127, 2020.

[3] T. Wang and Y. Tang, "Parallel deep reinforcement learning-based power flow state adjustment considering static stability constraint," *IET Gener. Transm. Distrib.*, vol. 14, no. 3, pp. 6276–6284, 2020.

[4] S. N. Okhuegbe, A. A. Ademola, and Y. Liu, "Newton–Raphson AC power flow convergence based on deep learning initialization and homotopy continuation," *IEEE Trans. Ind. Appl.*, 2024.

[5] X. Hu, J. Yang, Y. Gao, et al., "Adaptive power flow analysis for power system operation based on graph deep learning," *Int. J. Electr. Power Energy Syst.*, vol. 161, Art. no. 110166, 2024.

[6] X. Zhang, D. Li, and X. Fu, "A novel Wasserstein generative adversarial network for stochastic wind power output scenario generation," *IET Renew. Power Gener.*, vol. 18, no. 16, pp. 3731–3742, 2024.

[7] Y. Chen, X. Wang, and B. Zhang, "An unsupervised deep learning approach for scenario forecasts," in *Proc. 2018 Power Syst. Comput. Conf. (PSCC)*, Dublin, Ireland, 2018, pp. 1–7.

[8] Y. Chen, Y. Wang, D. Kirschen, et al., "Model-free renewable scenario generation using generative adversarial networks," *IEEE Trans. Power Syst.*, vol. 33, no. 3, pp. 3265–3275, 2018.

[9] Y. Zhang, Q. Ai, F. Xiao, et al., "Typical wind power scenario generation for multiple wind farms using conditional improved Wasserstein generative adversarial network," *Int. J. Electr. Power Energy Syst.*, vol. 114, Art. no. 105388, 2020, doi: 10.1016/j.ijepes.2019.105388.

[10] Y. Ma, M. Ma, N. Wang, et al., "Mid-term scenario generation for wind power using GAN with temporal-correlation enhancement block," *E3S Web Conf.*, vol. 6, Art. no. 01003, 2020.

[11] Y. Chen, P. Li, and B. Zhang, "Bayesian renewables scenario generation via deep generative networks," in *Proc. 52nd Annu. Conf. Inf. Sci. Syst. (CISS)*, Princeton, NJ, USA, Mar. 2018, pp. 1–6.

[12] J. Liang and W. Tang, "Sequence generative adversarial networks for wind power scenario generation," *IEEE J. Sel. Areas Commun.*, vol. 38, no. 1, pp. 110–118, 2020.

[13] R. Yu, W. Hu, H. Jiang, et al., "Research on scene generation method of wind and solar active power output based on k-medoids clustering and generative adversarial networks," in *Proc. 2021 11th Int. Conf. Power Energy Syst. (ICPES)*, Shanghai, China, 2021, pp. 690–695.

[14] S. Narayanan, R. Kumar, S. Ramadass, et al., "Innovative hybrid approach for enhanced renewable energy generation forecasting using recurrent neural networks and generative adversarial networks," *J. Electr. Eng. Technol.*, vol. 19, pp. 4847–4864, 2024.

[15] H. Muller, M. Rider, and C. Castro, "Artificial neural networks for load flow and external equivalents studies," *Electr. Power Syst. Res.*, vol. 80, no. 9, p. 10, 2024.

[16] Y. Yang, J. Yu, Z. Yang, et al., "Fast calculation of probabilistic optimal power flow: A deep learning approach," in *Proc. 2024 IEEE Power Energy Soc. Gen. Meeting (PESGM)*, 2024, pp. 1–5.

[17] M. Xiang, J. Yu, Z. Yang, et al., "Probabilistic power flow with topology changes based on deep neural network," *Int. J. Electr. Power Energy Syst.*, vol. 117, Art. no. 105650, 2024.

[18] P. Li, B. Yu, N. Chang, et al., "An efficient solution method for quadratic convex relaxation unit commitment in AC power flow based on binary neighborhood dynamic expansion," *Proc. Chin. Soc. Electr. Eng.*, pp. 1–19, accessed Nov. 13, 2025. [Online]. Available: https://link.cnki.net/urlid/11.2107.tm.20250616.0837.002

[19] J. Guo, S. Fan, Z. Cai, et al., "Human-machine hybrid enhanced intelligence in large power grid control: Conceptual connotation, application framework, key technologies, and system validation," *Proc. Chin. Soc. Electr. Eng.*, vol. 44, no. 17, pp. 6787–6811, 2024, doi: 10.13334/j.0258-8013.pcsee.241892.

[20] H. R. Baghaee, M. Mirsalim, and G. Gharehpetian, "Power calculation using RBF neural networks to improve power sharing of hierarchical control scheme in multi-DER microgrids," *IEEE J. Emerg. Sel. Topics Power Electron.*, vol. 4, no. 4, pp. 1217–1225, 2023.

[21] Z. Ma, Y. Li, X. He, et al., "A graph learning model for static security analysis of power grids based on power flow embedding and minimum cut pooling," *Southern Power Syst. Technol.*, vol. 19, no. 1, pp. 63–73, 92, 2025, doi: 10.13648/j.cnki.issn1674-0629.2025.01.007.

[22] M. Mirza and S. Osindero, "Conditional generative adversarial nets," *Computer Science*, vol. 1411, no. 1784, pp. 2672–2680, 2014.

[23] I. J. Goodfellow, J. Pouget-Abadie, M. Mirza, et al., "Generative adversarial networks," *Adv. Neural Inf. Process. Syst.*, vol. 3, pp. 2672–2680, 2014.

[24] S. Lee and I. H. T. Kim, "Exponentiated generalized Pareto distribution: Properties and applications towards extreme value theory," *Commun. Stat. Theory Methods*, vol. 48, no. 8, pp. 2014–2038, 2019.

[25] A. Al Mamun, M. Sohel, N. Mohammad, et al., "A comprehensive review of the load forecasting techniques using single and hybrid predictive models," *IEEE Access*, vol. 8, pp. 134911–134939, 2020.

[26] P. Pinson and R. Girard, "Evaluating the quality of scenarios of short-term wind power generation," *Appl. Energy*, vol. 96, pp. 12–20, 2012.

[27] X. Wang, Z. Hu, M. Zhang, et al., "Research on the construction of evaluation framework for short-term wind power scenario quality," *Power Syst. Technol.*, vol. 41, no. 5, pp. 1583–1589, 2017, doi: 10.13335/j.1000-3673.pst.2016.1985.